

# POWER SPECTRAL DENSITY OF DUAL RANDOMIZED DISCONTINUOUS PULSE WIDTH MODULATION

AIMAD BOUDOUDA<sup>1</sup>

**Keywords:** Random pulse width modulation (RPWM); Discontinuous pulse width modulation (DPWM); Switching losses; Electromagnetic Interference (EMI); Power spectral density; Voltage source inverter.

This paper addresses the spectral characteristics of a carrier-based dual randomized discontinuous pulse width modulation (DRDPWM) technique for reducing conducted EMI and switching losses in three-phase voltage source inverters. It combines two simple random schemes, random carrier frequency modulation (RCF-DPWM) and random pulse position modulation (RPP-DPWM). First, the modulating principle of the DRDPWM is presented. Then, the analytical expressions of power spectral density (PSD) that characterize the output voltage of the three-phase inverter are derived. Analytical and simulation results show the effectiveness of PSD spreading of the DRDPWM. Finally, experimental results verify the analytical and simulation results and prove the effectiveness of the DRDPWM scheme in spreading the spectrum compared to simple schemes (RPP-DPWM and RCF-DPWM) and conventional scheme DPWM.

## 1. INTRODUCTION

In the last decade, random pulse width modulation (RPWM) has shown to be a viable alternative to conventional PWM; it spreads the harmonics of the output voltage and current over a continuous noise spectrum with small amplitudes without increasing the switching frequency [1]. It has several benefits, such as improving compliance with EMC standards for EMI and mitigating acoustic noise in ASDs [2–4]. The existing simple random schemes that use only one random parameter are randomized carrier frequency modulation (RCFM) and randomized pulse position modulation (RPPM) [1–3,5–8]. However, for a maximum spreading of the voltage spectrum, the combination of the two schemes (RCFM-RPPM) has also been proposed [1, 9–15]. Most published works on random PWM techniques are based on continuous PWM. The literature shows only four publications on randomized discontinuous PWM [16–19]. They invariably randomize only one PWM parameter, for example, the pulse rate or the switching frequency. This paper proposes a carrier-based dual randomized discontinuous PWM technique (DRDPWM) to control a three-phase inverter. DRDPWM combines two simple random schemes, random pulse position modulation (RPP-DPWM) and random carrier frequency modulation (RCF-DPWM).

The proposed technique has the advantages of discontinuous PWM in terms of efficiency (reduced switching losses) and dual randomized PWM in EMC compliance (reduced EMI). This paper aims to develop a general analytical model for investigating the characteristic of the DRDPWM scheme and analyzes its effectiveness in spreading the output voltage spectrum. The model is expressed directly using the random parameters of the triangular carrier. The cases (DPWM, RPP-DPWM, and RCF-DPWM) can be deduced from the general model. The main contributions of this paper include the following:

1) In this paper, it is the first time that the randomization of two parameters is introduced in the discontinuous PWM technique, resulting in a combined or dual scheme (RPPRCF-DPWM). Simple schemes (RPP-DPWM, RCF-DPWM) can derive from the combined scheme.

2) This paper is the first time an analytical dual randomized DPWM model is derived.

3) Besides its advantage of low switching losses, DRDPWM has a more dispersed and continuously

distributed spectrum with significantly reduced amplitudes. This characteristic is an EMC advantage of the proposed scheme compared to simple random schemes (RPP-DPWM and RCF-DPWM) and the classical DPWM scheme.

The rest of the paper is organized as follows. First, we present the modulating principle of the proposed DRDPWM technique. Next, we present the analysis results of the output voltage analysis based on the analytical and estimated power spectral density using the Welch method. The results show that the DRDPWM scheme is the most effective in spreading the spectrum. Finally, experimental results confirm the analytical and simulation results and prove the effectiveness of the DRDPWM scheme in spreading the spectrum of output voltage compared to simple schemes (RPP-DPWM and RCF-DPWM).

## 2. DUAL RANDOMIZED DISCONTINUOUS PWM

Despite all the advantages of DPWM, its disadvantage is that harmonics at the switching frequency cause an electromagnetic interference (EMI) problem like all fixed switching frequency modulation techniques [17]. The random PWM technique is a good solution to overcome this problem. It allows spreading the output voltage harmonics over a continuous noise spectrum with small amplitudes without increasing the switching frequency. This provides several advantages, such as improved compliance with EMC restrictions [11,12,15]. The dual randomized discontinuous PWM technique, a new solution, is proposed to conserve the advantages of DPWM while adding those of the RPWM technique. Therefore, the proposed scheme allows for reducing the switching loss and reducing the EMI problem.

### 2.1. MODULATING PRINCIPLE

The structure of the converter is shown in Fig. 1. It requires three switching functions  $u_a$ ,  $u_b$  and  $u_c$ , which are obtained by comparing three deterministic discontinuous modulating functions  $r_a$ ,  $r_b$ , and  $r_c$ , to a randomized triangular carrier  $c$  (Fig. 2). Discontinuous modulating functions have gained special attention for their reduced-switching characteristics [16]. The most common carrier-based discontinuous modulating functions are DPWM0, DPWM1, DPWM2, and DPWM3 [20,21]. The DPWM0 was chosen as a case study in our work, as presented in Fig. 2. For each phase, the obtained switching function is characterized by three parameters: switching

<sup>1</sup> Laboratoire Ingénierie des Systèmes et Télécommunications (LIST), University M'Hamed Bougara, Avenue de l'indépendance, 35000, Boumerdes, Algeria, E-mail: a.boudouda@uiniv-boumerdes.dz

period  $T$ , delay report,  $\delta$ , and duty cycle  $d$ .

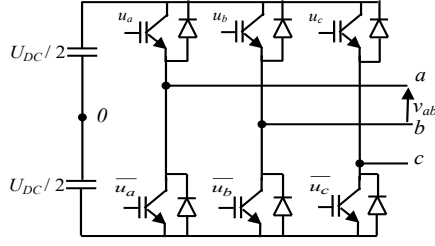


Fig. 1 – Three-phase inverter.

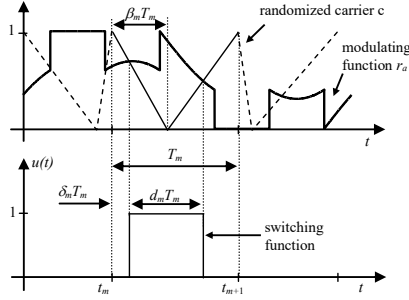


Fig. 2 – Modulating principle of DRDPWM technique

Theoretically,  $T$ ,  $\delta$  and  $d$  can be randomized in a combined or a separate way. In practice,  $d$  is obtained from a deterministic reference signal, thereby adjusting the output voltage. Therefore, only  $T$  and  $\delta$  are randomized. This can be obtained by a triangular carrier having two random parameters: the period  $T$  and the fall-time report  $\beta$ . The resulting random schemes are as follows:

- conventional discontinuous PWM (DPWM): The carrier is deterministic (parameters  $T$  and  $\beta$  fixed).
- randomized pulse position discontinuous PWM (RPP-DPWM): The carrier is randomized (fixed period  $T$  and randomized  $\beta$ ).
- randomized carrier frequency discontinuous PWM (RCF-DPWM): The carrier is randomized (randomized period  $T$  and fixed  $\beta$ ).
- combined random scheme: dual randomized pulse position carrier frequency discontinuous PWM (RPPRCF-DPWM): The carrier is randomized ( $T$  and  $\beta$  are simultaneously randomized).

Table 1  
Randomized discontinuous PWM schemes.

RDPWM Schemes	$\beta$	$T$
DPWM	fixed <sup>a</sup>	fixed
RPP- DPWM	randomized	fixed
RCF- DPWM	fixed <sup>a</sup>	randomized
RPPRCF- DPWM	randomized	randomized

a:  $\beta = 0$

In dc-ac, the reference signal  $r$  is an alternating signal between -1 and 1 such as a sinusoidal signal of amplitude less than or equal to 1. Thus, in practice while using a carrier  $c$  between 0 and 1 (Fig. 2), we need to return the reference  $r$  to the same scale as  $c$ , which gives:

$$r' = \frac{1}{2}(1 + r). \quad (1)$$

In addition, the dynamic of the reference is much lower than that of the carrier ( $F_s \gg F_1$ ;  $\overline{F_s}$  is the statistical mean of the switching frequency and  $F_1$  is the frequency of the reference  $r$ ), generally,  $r$  is updated once a switching period and for the

period  $T_m = t_{m+1} - t_m$  (Fig. 2), the resulting duty cycle ( $d_m$ ) depends on the random sampling instant  $t_m$ , giving:

$$d_m = d(t_m) = \frac{1}{2}(1 + r(t_m)), \quad (2)$$

and the delay report  $\delta_m$  can be expressed as follows:

$$\delta_m = \beta_m(1 - d_m). \quad (3)$$

For period  $T_m$ , randomized  $\beta_m$  between 0 and 1 leads to a random  $\delta_m$  between 0 and  $(1 - d_m)$ , then the timing of the PWM pulse varies between the beginning and the end of period  $T$ . In dc-ac, the use of  $\beta$  instead of  $\delta$  is paramount; it allows defining the pulse position regardless of the duty cycle  $d$ , which is varying in this case (Fig. 2). In addition, for a three-phase inverter, the randomization  $\beta$  gives randomized pulse position for the three switching functions.

Let's consider in Fig. 3, the switching function  $u_a(t)$  and the output voltage  $v_{a0}(t)$  in the general case of (DRDPWM) in which the switching period  $T$  and the delay report  $\delta$  are randomized.

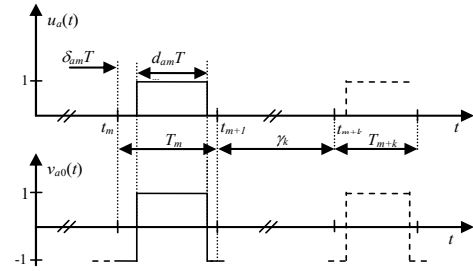


Fig. 3 – Output voltage and switching function.

Related to the switching function  $u_a$ , the per-unit phase to ground voltage  $v_{a0}$  is:

$$v_{a0}(t) = 2\left(u_a(t) - \frac{1}{2}\right), \quad (4)$$

and per unit phase-to-phase voltage  $v_{ab}$  is deduced easily:

$$v_{ab}(t) = v_{a0}(t) - v_{b0}(t) = 2(u_a(t) - u_b(t)), \quad (5)$$

$u_a$ ,  $u_b$  and  $u_c$  are obtained by comparing the reference signals  $r_a$ ,  $r_b$  and  $r_c$  to the carrier  $c$  as shown in (Fig. 2). Note that  $r_a$ ,  $r_b$  and  $r_c$  depend on the modulation strategy:

- Sine modulation (SM):

$$r_a = v_a^*, \quad (6)$$

$$v_a^*(t) = M \sin\left(2\pi \frac{t}{T_1}\right), \quad (7)$$

$T_1$  is the period of the reference signal and  $M$  is the modulation index: ( $0 \leq M \leq 1$ ). References  $r_b$  and  $r_c$  are shifted back and forth from  $r_a$  with an angle of  $(2\pi/3)$ rd.

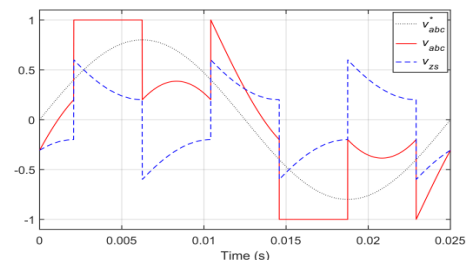


Fig. 4 – Modulation function of DPWM

- DPWM:

$$r_a = v_a^{***}, \quad (8)$$

For the three phases:

$$v_{abc}^{***} = v_{abc}^* + v_{zs}, \quad (9)$$

assume  $|v_a^*| \geq |v_b^*|, |v_c^*|$ , then:

$$v_{zs} = \left( \text{sign}(v_{abc}^*) \right) \frac{U_{dc}}{2} - v_{abc}^*. \quad (10)$$

The resulting reference signals for the two modulation strategies are given in Fig. 4.

## 2.2. SPECTRAL ANALYSIS OF THE DRDPWM TECHNIQUE

To evaluate the effectiveness of the proposed DRDPWM scheme in spreading the spectrum of the output voltage, an analysis with power spectral density (PSD) is used in this paper. Generally, the analysis of random signals can be performed either by fast Fourier transform (FFT) or by power spectral density (PSD). The FFT (which is originally discrete) leads to a continuous random spectrum, depending on the considered signal sample. Thus the (PSD) is more appropriate for such signals as it gives accurate results according to the Wiener-Khintchine theorem [5].

Based on the Wiener-Khintchine theorem, the PSD of a  $\tau$  long random signal  $u(t)$  is:

$$W(f) = \lim_{\tau \rightarrow \infty} \frac{1}{\tau} E \left[ |F\{u(t)\}|^2 \right], \quad (11)$$

where:

$F\{u(t)\}$ : Fourier transform of the signal  $u(t)$ .

$E[\cdot]$ : Statistical expectation.

### 2.2.1. ANALYTICAL EXPRESSION OF THE PSD BASED ON THE WIENER-KHINTCHINE THEOREM

For a wide sense stationary (WSS) pulse signal  $u(t)$ , (Fig. 3), a general expression of the PSD can be set as [5]:

$$W(f) = \frac{1}{T} \left\{ E \left[ |U_m(f)|^2 \right] + 2 \text{Re} \left( \sum_{k=1}^{\infty} E \left[ U_m(f) U_{m+k}^*(f) \right] \right) \right\} \quad (12)$$

where  $W(f)$  is the power spectral density,  $U_m(f)$  is the Fourier transform of the signal  $u_{Tm}(t)$  during the switching period  $T_m$ ,  $U_{m+k}^*(f)$  is the complex conjugate of  $U_{m+k}(f)$ ,  $\bar{T}$  is the statistical mean of the switching period  $T$ ,  $E[\cdot]$  is the statistical expectation, and  $\text{Re}(\cdot)$  is the real part.

For phase a, the Fourier transform of the switching function of Fig. 3 is

$$U_{am}(f) = \frac{1}{\pi f} e^{-j\pi f(2\delta_{am} + d_{am})T_m} \sin(\pi f d_{am} T_m) e^{-j2\pi f t_m} \quad (13)$$

where  $d_{am}$  is the duty cycle given by eq. (2),  $\delta_{am}$  is the delay report given by eq. (3).

In dc-ac conversion, the duty cycle  $d$  depends upon the sampling instant  $t_m$  (i.e., beginning of the switching period). The switching function can't be considered a wide-sense stationary signal [1,9,12]. To obtain a broad sense stationary signal, the duty cycle  $d$  should be expressed as follows:

$$d_{am} = d_a(t_m) = \frac{1}{2} \left( 1 + r_a(t'_m, \theta) \right), \quad (14)$$

where  $t'_m = (m-1)\bar{T}$ ,  $\theta$  is an additional random parameter between 0 and  $2\pi$ .  $\tau$  represents the total uncertainty about the time reference of the modulating function. Expression (14) implies the periodicity of the duty cycle:

$$d_a(t'_m + lT_1, \theta) \approx d_a(t'_m, \theta) \quad (15)$$

where  $T_1$  is the period of the modulating function, and  $l$  is an

arbitrary integer.

Knowing that the two parameters  $T$  and  $\beta$  are independently randomized, general expressions of phase-to-ground voltage  $v_{a0}$  and phase-to-phase voltage  $v_{ab}$  PSDs can be set based on the:

- Relations (4) and (5) between switching functions and output voltages.

- General expression (12) of a pulse signal PSD.

- Bech's approximation, which assumes the random value of lag time  $\gamma_k$ , (Fig. 3) to be equal to its' statistical expectation [5]:

$$\gamma_k = t_{m+k} - t_{m+1} \approx (k-1)\bar{T}, \quad (16)$$

### A. PSD OF PHASE-TO-GROUND VOLTAGE

In expression (17) below, the random aspects of  $T$  and  $\beta$  are clearly separated, which allows distinguishing RPP-DPWM and RCF-DPWM schemes [1]:

$$W_a(f) \approx \frac{\varepsilon}{\bar{T}(\pi f)^2} E_{\theta, T_m} \left[ \sin^2(\pi f d_a(0, \theta) T_m) \right] + \frac{2\varepsilon}{\bar{T}(\pi f)^2} \text{Re} \left\{ \sum_{k=1}^N \left[ \begin{array}{l} E_{T_m} \left[ \begin{array}{l} \sin(\pi f d_a(0, \theta) T_m) e^{j\pi f(2-d_a(0, \theta)) T_m} \\ \times E_{\beta_m} \left[ e^{-j2\pi f \beta_m(1-d_a(0, \theta)) T_m} \right] \end{array} \right] \\ E_{\theta} \left[ \begin{array}{l} \sin(\pi f d_a(k\bar{T}, \theta) T_{m+k}) e^{j\pi f d_a(k\bar{T}, \theta) T_{m+k}} \\ \times E_{T_{m+k}} \left[ \begin{array}{l} \sin(\pi f d_a(k\bar{T}, \theta) T_{m+k}) e^{j\pi f d_a(k\bar{T}, \theta) T_{m+k}} \\ \times E_{\beta_{m+k}} \left[ e^{j2\pi f \beta_{m+k}(1-d_a(k\bar{T}, \theta)) T_{m+k}} \right] \end{array} \right] \end{array} \right] \\ \times E_T \left[ e^{j2\pi f T} \right]^{k-1} \end{array} \right\} \times \left( 1 - E_T \left[ e^{j2\pi f T} \right]^N \right)^{-1} \quad (17)$$

where  $\varepsilon = 1$  for  $f = 0$  and  $\varepsilon = 2$  otherwise and  $\theta$  is a random variable between 0 and  $2\pi$ ,  $N = \text{round}(T_1/\bar{T})$ .

### B. PSD OF PHASE-TO-PHASE VOLTAGE

Although the expression (18) of the PSD is more complicated, the two expectations on  $T$  and  $\beta$  are still well separated [1]

$$W_{ab}(f) \approx \frac{2}{\bar{T}(\pi f)^2} E_{\theta, T_m} \left[ \begin{array}{l} \sin^2(\pi f d_a(0, \theta) T_m) + \sin^2(\pi f d_b(0, \theta) T_m) \\ - 2 \sin(\pi f d_a(0, \theta) T_m) \sin(\pi f d_b(0, \theta) T_m) \\ \times E_{\beta_m} [\cos(\pi f(1-2\beta_m)(d_a(0, \theta) - d_b(0, \theta)) T_m)] \end{array} \right] + \frac{4}{\bar{T}(\pi f)^2} \text{Re} \left\{ \sum_{k=1}^N \left[ \begin{array}{l} E_{T_m} \left[ \begin{array}{l} \sin(\pi f d_a(0, \theta) T_m) e^{j\pi f(2-d_a(0, \theta)) T_m} \\ \times E_{\beta_m} \left[ e^{-j2\pi f \beta_m(1-d_a(0, \theta)) T_m} \right] \\ - \sin(\pi f d_b(0, \theta) T_m) e^{j\pi f(2-d_b(0, \theta)) T_m} \\ \times E_{\beta_m} \left[ e^{-j2\pi f \beta_m(1-d_b(0, \theta)) T_m} \right] \end{array} \right] \\ E_{\theta} \left[ \begin{array}{l} \sin(\pi f d_a(k\bar{T}, \theta) T_{m+k}) e^{j\pi f d_a(k\bar{T}, \theta) T_{m+k}} \\ \times E_{T_{m+k}} \left[ \begin{array}{l} e^{j2\pi f \beta_{m+k}(1-d_a(k\bar{T}, \theta)) T_{m+k}} \\ - \sin(\pi f d_b(k\bar{T}, \theta) T_{m+k}) e^{j\pi f d_b(k\bar{T}, \theta) T_{m+k}} \\ \times E_{\beta_{m+k}} \left[ e^{j2\pi f \beta_{m+k}(1-d_b(k\bar{T}, \theta)) T_{m+k}} \right] \end{array} \right] \end{array} \right] \\ \times E_T \left[ e^{j2\pi f T} \right]^{k-1} \end{array} \right\} \times \left( 1 - E_T \left[ e^{j2\pi f T} \right]^N \right)^{-1} \quad (18)$$

### C. PARTICULAR CASES: RCF-DPWM AND RPP-DPWM SCHEMES

Note that the expectations related to  $T$  and  $\beta$  are well separated in eq. (17) and (18), which allows distinguishing the simple schemes RPPM and RCFM as follows:

- RPP-DPWM scheme: fixed period  $T$  and randomized  $\beta$ .
- RCF-DPWM scheme: randomized  $T$  and fixed  $\beta$ : ( $\beta = 0.5$ ).

### 2.2.2. ESTIMATED POWER SPECTRAL DENSITY BASED ON WELCH APPROXIMATION

To reinforce the validity of analytical and experimental results, a numerical estimation method of the PSD called Welch's method is used [22]. The estimated PSD is

computed by applying Welch's method to a sample of the considered signals got experimentally or by simulation (output voltage, current). The obtained signals are sampled using a digital oscilloscope or the A/D converter with a sampling time of  $T_s$ , and then the power spectral density can be computed offline by using MATLAB [23].

It gives very satisfactory results compared to analytical and measurement ones [1, 11, 12, 15]. Welch's method is the core function of most digital signal analyzers (DSA). The Welch's estimation method is implemented in the signal processing toolbox of MATLAB by the pwelch function [23]:  $PSD = \text{pwelch}(X, \text{Window}, \text{Noverlap}, \text{NFFT}, \text{Fs})$  where  $X$  is the discrete-time signal vector (sampled data); Window is the window function applied to segments; Noverlap is the number of overlapped samples; NFFT is the number of discrete FFT samples used to calculate the estimated PSD, and  $Fs$  is the sampling frequency.

### 2.2.3. RANDOMIZATION OF THE TRIANGULAR CARRIER SIGNAL

The key point of randomized PWM techniques is how to generate random numbers [10]. To randomize the triangular carrier's modulation parameters ( $T$  and  $\beta$ ), we use the pseudo-random number generator PRNG available as a MATLAB utility. In our work, we adopted a pseudo-random number generator function (genrand) based on the algorithm of Mersenne twister [24].

The lower limits ( $T_{\min}$ ,  $\beta_{\min}$ ) and upper limits ( $T_{\max}$ ,  $\beta_{\max}$ ) of the random parameters  $T$  and  $\beta$  are defined by the following randomness levels  $R_T$  and  $R_\beta$ , respectively:

$$\text{for RCFM: } R_T = \frac{T_{\max} - T_{\min}}{\bar{T}}, \quad (19)$$

$$T \in \left[ \bar{T} \left( 1 - \frac{R_T}{2} \right), \bar{T} \left( 1 + \frac{R_T}{2} \right) \right], \quad (20)$$

where  $\bar{T}$  is the statistical mean of switching period  $T$ .

$$\text{for RPPM: } R_\beta = \frac{\beta_{\max} - \beta_{\min}}{\bar{\beta}}, \quad (21)$$

$$\beta \in \left[ \bar{\beta} \left( 1 - \frac{R_\beta}{2} \right), \bar{\beta} \left( 1 + \frac{R_\beta}{2} \right) \right], \quad (22)$$

where  $\bar{\beta} = 0.5$  is the statistical mean of the delay report  $\beta$ .

The random parameters  $T$  and  $\beta$  may take any probability law. We use the uniform law in our work because it's the simplest to implement. Thus, we express the instantaneous switching period  $T$  and the delay report  $\beta$  as follows:

$$\begin{cases} T = T_{\min} + (T_{\max} - T_{\min}) \times R \\ \beta = \beta_{\min} + (\beta_{\max} - \beta_{\min}) \times R \end{cases} \quad (23)$$

$R$ : is a series of uniformly distributed random numbers in the interval  $[0, 1]$  and generated by using the pseudo-random number generator function (genrand).

Replacing  $(T_{\max} - T_{\min})$  and  $(\beta_{\max} - \beta_{\min})$  by their values (19) and (21) respectively in (23), we get:

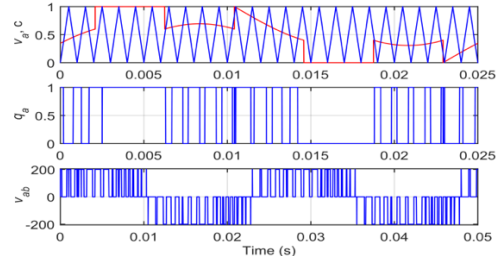
$$\begin{cases} T = T_{\min} + \bar{T} R_T R \\ \beta = \beta_{\min} + \bar{\beta} R_\beta R \end{cases} \quad (24)$$

## 3. ANALYTICAL AND SIMULATION RESULTS

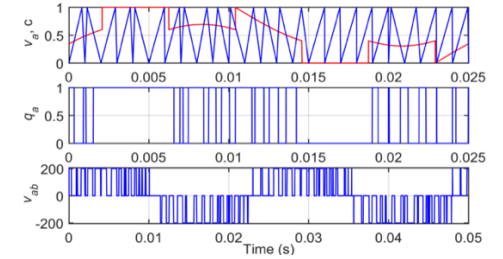
In this section, we will verify the proposed DRPWM technique using the analytical expression of the PSD and numerical

estimation of the PSD-based-Welch method. The estimated PSD is computed by the application of Welch's method on a sample of the output voltage and current, after simulation of the inverter-fed induction motor. The PSD analysis is performed using the following modulation parameters:

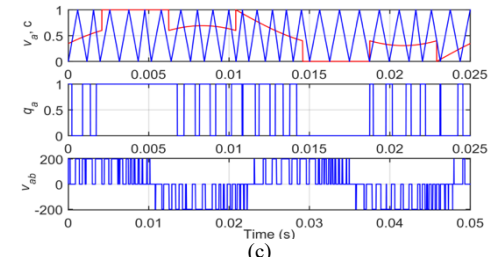
- Input voltage:  $U_{dc} = 200$  V.
- Load: ( $R = 65 \Omega$ ,  $L = 70$  mH) provide a load angle of  $15.14^\circ$
- Random triangular carrier: the intervals of randomization of parameters  $T$  and  $\beta$  are obtained with  $R_T = 0.2$  and  $R_\beta = 1.2$ .
- The uniform probability density function is used for all randomizations.
- Reference signal: discontinuous modulating function DPWM0 of fundamental frequency  $f = 40$  Hz, modulation index  $M = 0.8$ .
- The parameters of Welch's method are given in Appendix A (see Table A1).



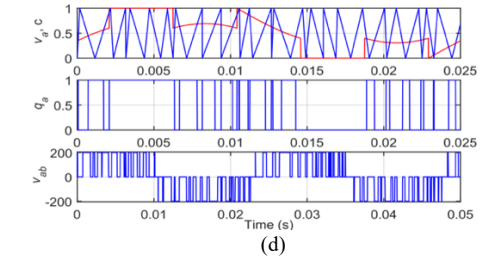
(a)



(b)



(c)



(d)

Fig. 5 – Simulated waveforms of triangular carrier and modulating function (upper trace), switching signals  $u_a$  (middle trace), output voltage  $v_{ab}$  (lower trace) ( $f_c = 1$  kHz,  $M = 0.8$ ,  $R_T = 0.2$ ,  $R_\beta = 1.2$ ), (a) DPWM, (b) RPP-DPWM, (c) RCF-DPWM, (d) RPPRCF-DPWM

Figure 5 presents the waveforms of triangular carrier and modulating function, switching signals  $u_a$ , phase-to-phase voltage ( $v_{ab}$ ), respectively, for the four schemes: DPWM, RPP-DPWM, RCF-DPWM, and RPPRCF-DPWM. The figures clearly show that the proposed modulating scheme gives fewer switching losses.

Figure 6 shows computed and estimated PSDs of phase-to-phase voltage ( $v_{ab}$ ) for the four schemes: DPWM, RPP-DPWM, RCF-DPWM, and RPPRCF-DPWM, respectively. Note that the deterministic scheme DPWM is taken as a benchmark. A perfect agreement between the analytical PSD and the estimation is obtained for all schemes (DPWM, RPP-DPWM, RCF-DPWM, and RPPRCF-DPWM).

In the DPWM scheme, as shown in Fig. 6(a), the spectrum comprises discrete power harmonics with important amplitudes clustered around the switching frequency ( $f_s = 1$  kHz) and its multiples.

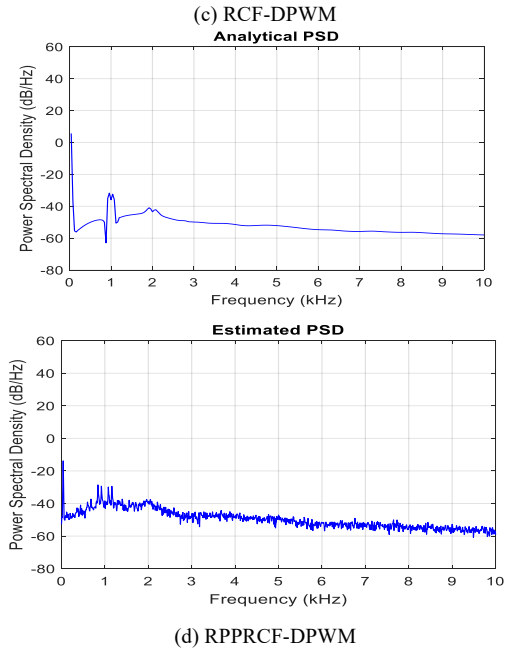
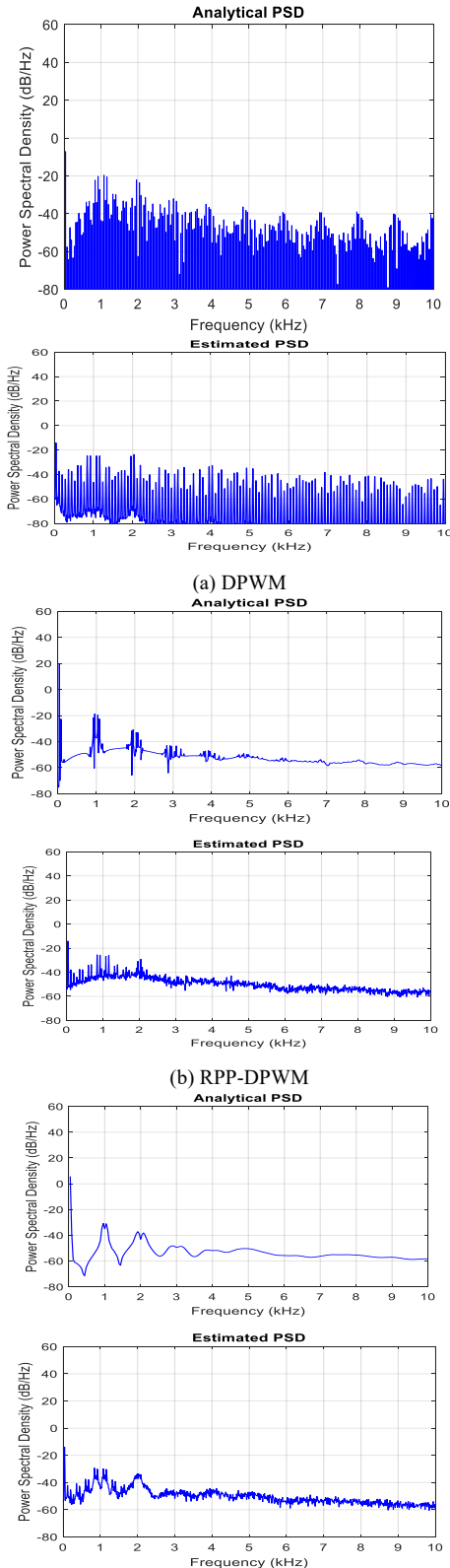


Fig. 6 – PSD of phase-to-phase voltage ( $f_s = 1$  kHz,  $f = 40$  Hz,  $M = 0.8$ , X-axis: 1 kHz/div., Y-axis: 20 dB/div.)

In Fig. 6(b), the RPP-DPWM scheme cannot spread the PSD completely; it has a continuous part (noise) and a discrete one (power harmonics). In Fig. 6(c), the RCF-DPWM scheme gives a completely spread PSD that considerably reduces the amplitude of the peaks. Therefore, the RCF-DPWM is more efficient than the RPP-DPWM. However, Fig. 6(d) shows that the proposed scheme (RPPRCF-DPWM) provides the most spread PSD compared to RCF-DPWM and RPP-DPWM; it reduced the PSD peaks around the modulation frequency ( $f_s = 1$  kHz) by 6 dB and around ( $2f_s = 2$  kHz) by 12 dB. Moreover, this reduction is more important at higher frequencies. This advantage is expected as the proposed scheme combines the properties of the two simple schemes (RCF-DPWM and RPP-DPWM).

## 4. EXPERIMENTAL RESULTS

### 4.1. EXPERIMENTAL SETUP

Figure 7 shows the experimental setup used for testing the proposed scheme, as discussed above. We have implemented all the schemes of the random DPWM technique using the rapid prototyping and real-time interface system dSPACE with DS1104 control board (A TMS320F240 from Texas Instruments).

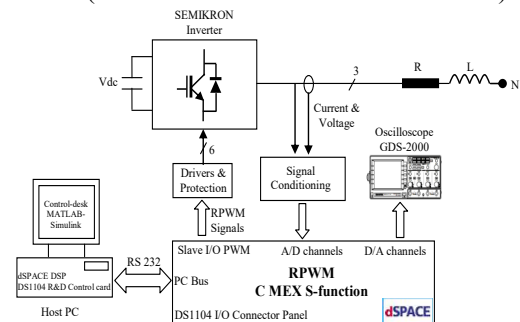


Fig. 7 – Block diagram of the experimental setup

The experimental setup is equipped with a three-phase resistive-inductive load. A 2-level SEMIKRON inverter feeds the load. The DC supply voltage is  $U_{dc} = 200$  V. A 4-Channel digital storage oscilloscope (INSTEK GDS-2204) is

used for real-time measurements. The voltage is measured using Hall-effect sensors type LEM (LA55-P).

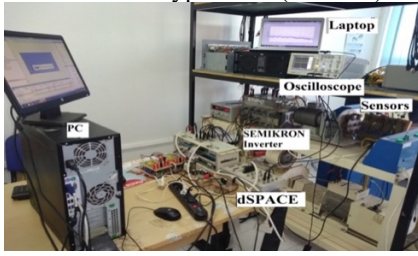


Fig. 8 – Photograph of the experimental setup.

Figure 9 shows the measured waveforms of the triangular carrier signal and the corresponding switching signals for all RDPWM schemes, while the conventional DPWM is taken as a benchmark. The randomness of the triangular and switching signals appears clearly for all RDPWM schemes.

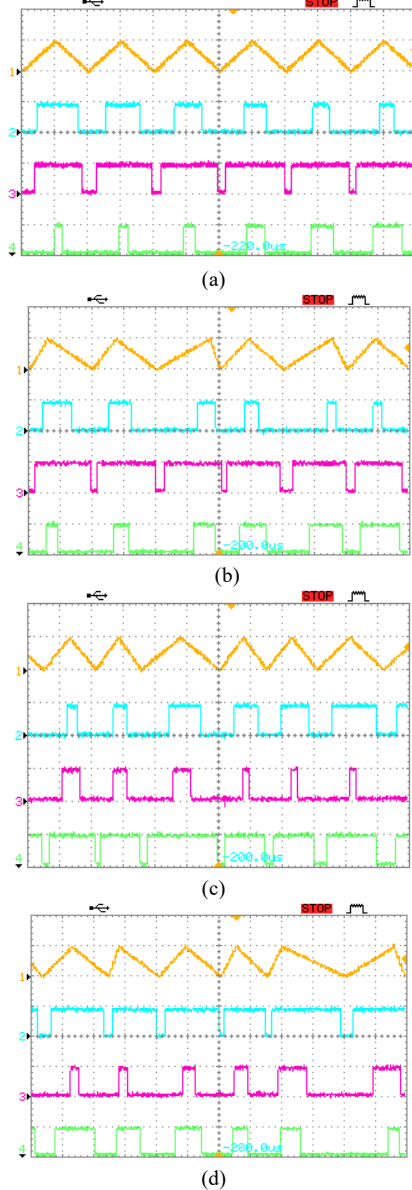


Fig. 9 – Measured waveforms of the triangular carrier (upper trace) and switching signals for the three legs (lower trace) ( $f_s = 1$  kHz,  $M = 0.8$ ,  $R_T = 0.2$ ,  $R_\beta = 1.2$ ), (a) DPWM, (b) RPP-DPWM, (c) RCF-DPWM, (d) RPPRCF-DPWM

#### 4.2. PSD ANALYSIS OF THE OUTPUT VOLTAGE

Figure 10 shows the measured PSDs of phase-to-phase

voltage ( $v_{ab}$ ) for DPWM, RPP-DPWM, RCF-DPWM, and RPPRCF-DPWM schemes. Despite the limited frequency resolution, all measurements are consistent with the analytical and simulation results. Hence, they validate the theory and prove the effectiveness of implementation with dSPACE.

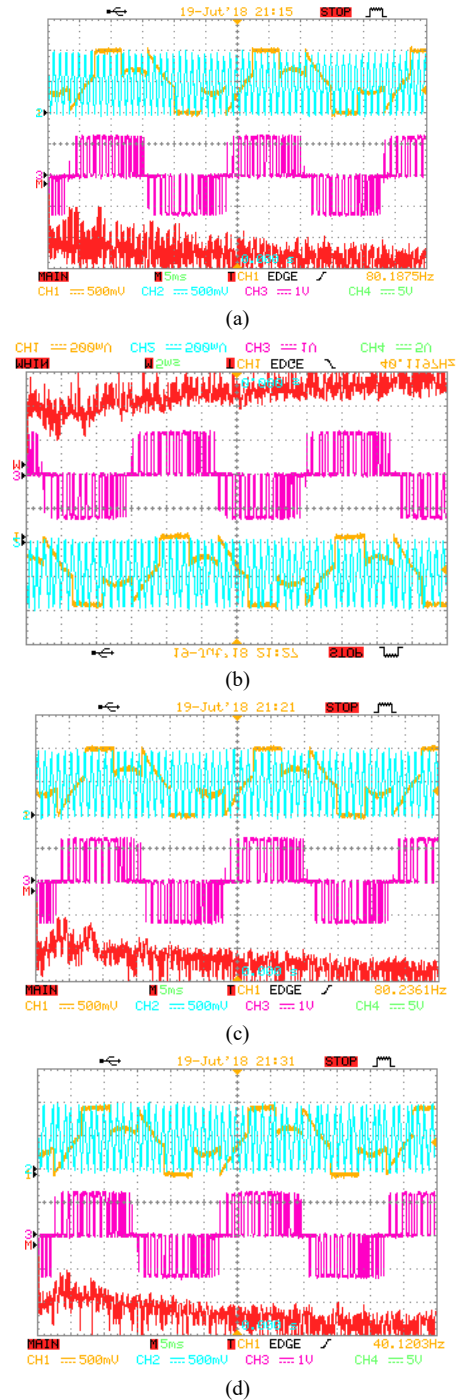


Fig. 10 – Measured PSD of phase-to-phase voltage, ( $f_s = 1$  kHz,  $f = 40$  Hz,  $M = 0.8$ , X-axis: 845 Hz/div., Y-axis: 20 dB/div.), (a) DPWM, (b) RPP-DPWM, (c) RCF-DPWM, (d) RPPRCF-DPWM

To illustrate the results quantitatively, the decrease in amplitudes for random schemes is presented in Table 2. The (RCFM-RPPM) scheme significantly reduces harmonic amplitudes compared to other schemes (RPPM and RCFM). It reduces the peaks of the power spectral density (PSD) around the modulation frequency ( $f_s = 1$  kHz) by 10 dB and around ( $2f_s = 2$  kHz) by 16 dB. Moreover, this reduction is more important at higher frequencies.

Table 2  
Comparative summary of different random schemes

RPWM schemes	Mesured PSD (dB/Hz)		
	$f_s$	$2f_s$	$3f_s$
DPWM	-20	-19.99	-32
RPP- DPWM	-21.47	-26.63	-39.53
RCF- DPWM	-30.48	-31.75	-44.54
RPPRCF- DPWM	-30.46	-36.53	-45.82

## 5. CONCLUSIONS

This paper proposes a carrier-based dual randomized discontinuous pulse width modulation (DRDPWM) to control a three-phase inverter. DRDPWM combines a random carrier frequency (RCF-DPWM) scheme and a random pulse position (RPP-DPWM) scheme. In addition to the performances of the proposed DRDPWM in reducing the switching losses, it allows a better spread of the spectrum with significantly reduced amplitudes, which is an EMC advantage. The analytical, simulation, and experimental results clearly show the proposed method's effectiveness in spreading the output voltage spectrum compared to other simple and conventional deterministic techniques.

## APPENDIX A

The settings of the Pwelch function used in this study are given in Table A1.

Table A1  
Settings of the Welch's method.

Spectrum units	dB/Hz
Sampling frequency	38.460 kHz
Window type	Hamming
Record length	10,000 samples
Window length	2000 samples
Segments number	5 segments
Overlap percentage	20 %

Received on 10 October 2022

## REFERENCES

- N. Boudjerda, A. Boudouda, M. Melit et al, *Spread spectrum in three-phase inverter by an optimised dual randomised PWM technique*, Int. J. Electron. **101**, pp. 308-324 (2014).
- Y., Li, H. Wu, Q. Si, Y.G., Liu, *Vibration noise suppression approach based on random switching frequency (RSF) Control for Permanent Magnet Motor*, Trans. Can. Soc. Mech. Eng. **45**, pp. 444-460 (2020).
- F. Mihali, D. Kos, *Reduced conductive EMI in switched-mode DC-DC power converters without EMI filters: PWM versus randomized PWM*, IEEE Trans. Power Electron. **21**, pp. 1783-1794 (2006).
- P. Lezynski, *Random modulation in inverters with respect to electromagnetic compatibility and power quality*, IEEE Trans. Emerg. Sel. Topics Power Electron. **6**, pp. 782-790 (2017).
- R.L. Kirlin, M.M. Bech, A.M. Trzynadlowski, *Analysis of power and power spectral density in PWM inverters with randomized switching frequency*, IEEE Trans. Ind. Electron. **49**, pp. 486-499 (2002).
- Z. Zhang, L. Wei, P. Yi, Y. Cui, P.S. Murthy, A.M. Bazzi, *Conducted Emissions Suppression of Active front end (AFE) drive based on random switching frequency PWM*, IEEE Transactions on Industry Applications, **56**, 6, pp. 6598-6607, (2020).
- C.-H. Moon, C.-J. Chen, S.-W. Lee, *A random modulation spread-spectrum digital PWM for a low system clock digital buck converter*, IEEE Access, **9**, pp. 156663-156671 (2021).
- T. Pan, H. Wu, C. Fu, D. Wu, *Novel random pulse position modulation for three-phase four-leg inverters*, Proceedings of the Institution of Mechanical Engineers, Part I: Journal of Systems and Control Engineering, **232**, 5, pp. 541-549 (2018).
- K.El K. Drissi, P.C.K. Luck, B. Wang et al, *A novel dual-randomization PWM scheme for power converters*, Proc. of IEEE PESC'03, Acapulco, Mexicopp, pp. 480-484 (2003).
- K. Kim, Y. Jung, Y. Li, *A new hybrid random PWM scheme*, IEEE Trans. Power Electron. **24**, pp.192-200, (2009).
- A. Boudouda, N. Boudjerda, D.K. El Khamlichi et al, *Combined random space vector modulation for a variable speed drive using induction motor*, Electr. Eng., Archiv für Elektrotechnik. **98**, pp.1-15, (2016).
- A. Boudouda et al., *Dual randomized pulse width modulation technique for buck converter fed by photovoltaic source*, Rev. Roum. Sci. Techn.–Électrotechn. et Énerg., **63**, 3, pp.289-294, (2018).
- F. Bu, T. Pu, W. Huang and L. Zhu, *Performance and evaluation of five-phase dual random SVPWM strategy with optimized probability density function*, IEEE Transactions on Industrial Electronics, **66**, 5, pp. 3323-3332, (2019).
- Y. Huang, Y. Xu, W. Zhang et al, *Hybrid RPWM technique based on modified SVPWM to reduce the PWM acoustic noise*, IEEE Trans. Power Electron. **34**, pp.5667-5674, (2019).
- A. Boudouda, A. Bouzida, F. Nafa, *Spectral analysis of switch voltage for dual randomized PWM dc-dc converters operating in DCM*. Int. J. Electron. Lett., **10**, 1, pp. 101-114, (2022).
- A. Trzynadlowski, R. L. Kirlin, S. Legowski, *Space vector PWM technique with minimum switching losses and variable pulse rate*, IEEE Trans. Ind. Electron., **44**, 2, pp. 173-181, (1997).
- K. H. E. Miliani and K. E. K. Drissi, *Discontinuous random space vector modulation for electric drives: A digital approach*, IEEE Trans. Power Electron., **27**, 12, pp. 4944-4951, (2012).
- S. Bhattacharya, D. Mascarella, G. Joos, G. Moschopoulos, *Reduced Switching Random PWM Technique for Two-level Inverters*, IEEE 2015 Energy Conversion Congress and Exposition (ECCE), pp. 695-202 (2015).
- Z. Zhang, L. Wei, P. Yi, P.S. Murthy, Y. Cui, *Optimized digital implementation of carrier-based randomized discontinuous PWM technique for active front end (AFE) drives*, 2019 IEEE Energy Conversion Congress and Exposition (ECCE), pp. 4390-4394 (2019).
- S.-A. Touil, Na. Boudjerda, A. Boubakir, K. El K. Drissi, *Closed Loop Discontinuous Pulse Width Modulation Control Used In Inverter Grid-Connected Photovoltaic System For Reduced Switching Losses*, Rev. Roum. Sci. Techn.–Électrotechn. et Énerg., **64**, 4, pp. 357-363 (2019).
- T. Fadaeian, S.A. Gholamian, H. Ghoreishy, *A novel discontinuous pulse width modulation strategy based on circuit-level decoupling concept for Vienna rectifier*, Rev. Roum. Sci. Techn.–Électrotechn. et Énerg., **65**, 1-2, pp. 87-95 (2020).
- P. Welch, *The use of fast Fourier transform for the estimation of power spectra: a method based on time averaging over short, modified periodograms*, IEEE Trans. Audio and Electroacoust., **15**, pp. 70-73 (1967).
- \*\*\*Matlab (2004) Signal Processing Toolbox. The Math Work Inc., Natick, MA.
- M. Matsumoto, T. Nishimura, *Mersenne twister: a 623- dimensionally equidistributed uniform pseudo-random number generator*, ACM Trans. Model. Comput. Simul., **8**, pp. 3-30 (1998).